

THREE-STEP MODEL OF DISPERSED FLOW HEAT TRANSFER (POST CHF VERTICAL FLOW)

by

O.C. Iloeje*, W. M. Rohsenow++ and P. Griffith++

*Department of Mechanical Engineering, University of Nigeria, Nsukka.

++Department of Mechanical Engineering, MIT, Cambridge, Massachusetts.

ABSTRACT

The paper presents a three step model of the dispersed flow heat transfer process, using an analysis of a single drop motion and heat transfer, and a statistical representation of the overall behaviour of the drops. The resulting equation gives the total heat transferred to the flow in terms of the mass flux, flow quality, fluid properties, wall roughness, and wall superheat. It includes the effect of contact angle or change in the wet ability of the surface. The range of validity of the model and the equation extends from dry wall film boiling to transition boiling, and is limited on the low temperature end by the critical Heat Flux region. Since the equation is analytically derived, its differentiation with respect to wall superheat will yield the Minimum Heat Flux point. The equation and model provide a very powerful base for analysis and prediction of post Critical Heat Flux heat transfer. The stable film boiling data for dispersed vertical flow of liquid nitrogen from reference [1] have been compared with the prediction and the results have been favourable.

NOMENCLATURE

| | |
|-------------------|---|
| a, b | constants |
| C | constant |
| CHF | critical heat flux |
| \bar{C} | mean drop concentration(kg/s-m ²) |
| c | specific heat at constant pressure (KJ/kg k) |
| D | channel diameter (m) |
| E | kinetic energy (Nm) |
| F | force (N) |
| f | friction factor |
| G | axial mass flux (kg/s-m ²) |
| g | gravitational acceleration (m/s ²) |
| h_{fg} | enthalpy of evaporation (kJ/kg) |
| K | drop transfer coefficient (m/s) |
| k | thermal conductivity (W/m-k) |
| M | drop deposition mass flux (kg/s-m ²) |
| m | drop mass (kg) |
| \dot{m} | mass flow rate (kg/s) |
| N | Numerical drop flux (s ⁻¹ m ⁻²) |
| n | integer 1,2,3, |
| P | pressure (N/m ² , bar) |
| P^f | penetration fraction |
| $P(E_1 \geq E_2)$ | probability distribution function |
| Pr | Prandtl Number |
| q/A, q" | Heat flux (W/m ²) |
| R_v | gas constant |
| Re; r | Reynolds Number; drop radius (m) |
| T | Temperature (K) |
| t | Time (s) |
| t_1 | dimensionless relaxation $t_1 J_{be} = V^2 \beta / V_v$ |
| a | radial velocity of vapor between drop and wall (m/s) |
| V | velocity (m/s) |
| V^* | friction velocity (m/s) |
| V_t | dimensionless drop deposition velocity = V_d / V^* |
| X | quality. |

| | |
|---|---|
| x | radial coordinate between drop and wall (m) |
| Y | distance normal to wall (m) |
| Z | axial distance (m) |

Greek Symbols

| | |
|---------------|--|
| ρ | density (kg/m ³) |
| δ | drop diameter (m) |
| σ | surface tension (N/m) |
| β | particle relaxation time = $2/9 \rho p r^2 / v_v$ (s) |
| ν | kinematic viscosity (m ² /s) |
| μ | dynamic viscosity (kg/m-s) |
| α | void fraction |
| Υ | fraction of drops, deposited at thermal boundary layer, which reach the wall |
| θ | truncation angle |
| ε | wall roughness |
| α_t | thermal diffusivity (m ² /s) |
| ϕ | heat transfer per unit area (kJ/m ²) |
| φ | quantity of heat (kJ) |
| ΔT | temperature difference (K) |
| λ | constant |

Subscript

| | |
|--------------|--|
| bv, vb | bulk vapour |
| bl | at thermal. boundary layer |
| c | contact |
| cp | conduction path |
| d | drop deposition |
| dc | drop contact |
| i(= 0,1 - 4) | indices for constant C |
| L | liquid |
| m | mean |
| min | minimum |
| n | normal to wall |
| ndc | non drop contact |
| P | particle |
| s | saturation |
| v | vapor |
| vf | vapor film temperature, $T_f = 1/2 (T_w + T_s)$ |
| w | wall; waD superheat; ' corresponding to wall temperature |
| wm | mean of distribution between $E = 0$ and $E = E_w$ |
| wv | wall to bulk vapor |
| δ | drop |

INTRODUCTION

Dispersed flow boiling in which the liquid drops are discretely distributed through a continuous vapour phase, is characteristic of Post Critical Heat Flow heat transfer. It occurs most frequently in boilers that deliver superheated vapour, and considerable interest is centred on the phenomena in the analysis of heat transfer from, and heat up of, fuel rods in Nuclear Reactors (BWR or PWR) in the event of a loss of coolant accident.

The standard boiling curve for a given quality mass flux and pressure set, is illustrated in figure 1. In

the Post Critical Heat Flux region, two distinct sections are obvious, viz, transition and stable film boiling regions. In the former region, the heat flux from wall to the flow deteriorates with wall superheat increasing, while the converse is true for the latter. This and other differences in behaviour have raised the question as to whether the boiling process processes in the two regions are fundamentally different. The dispersed flow boiling model developed in this paper will show that the boiling process are in fact, the same. The minimum

heat flux point merely represents a point transfer, over heat transferred from wall to the bulk ascendency of direct drop-wall contact heat vapour and the liquid drops not touching the wall,

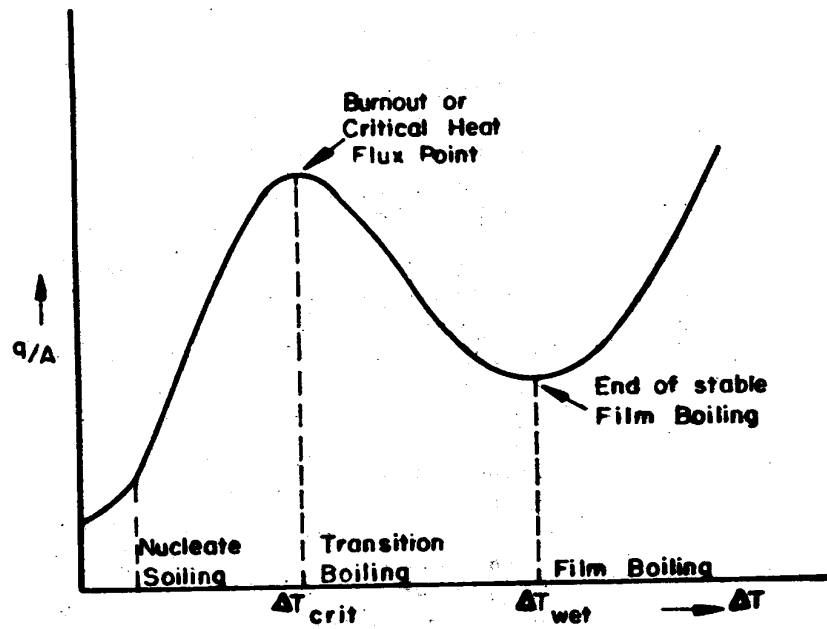


Figure 1: Full Boiling Curve

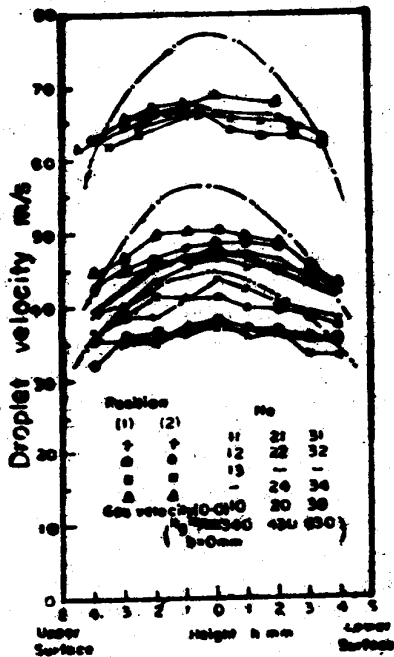


Figure 2a: Axial velocity of drops in air/water

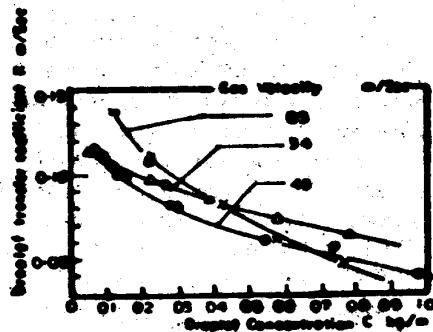


Figure 2b: Droplet transfer coefficients (ref. 5)

while going from the high to the low wall temperature boiling regions

The objectives of this paper are to present:

- a) a structural description of the post CHF dispersed flow boiling process,
- b) a heat transfer model derived from (a) above, leading to an analytic expression for the total heat flux from wall to fluid,
- c) a comparison of the relation from (b) against known trends of the boiling curve and against available liquid nitrogen data in the film boiling region.

POST CHF DISPERSED FLOW AND BOILING

The liquid drops in dispersed flow have random velocities imparted to them by the energy in the mean flow. For axial slip ratios, V_v/V_L between 1 and 2, the axial velocities of the drops are fairly uniform across the channel, figure 2a. With heat addition, vapour acceleration due to the evaporation process accelerates the drop until the Weber Number, $\rho\delta(V_v/V_L)^2/\sigma$, reaches 3 critical value. The drop then breaks up into two or more drops. The droplet breakup process has been analysed and introduced into dispersed flow film boiling modelling, with success, by Forslund [2], and Hynek, Rohsenow, and Bergles [3]. In so far as the drop velocity component normal to and towards the wall determines the deposition rate and penetration liquid drops towards the hot wall, it is fundamental to the determination of the contribution of liquid drops to the overall heat transfer from the wall. The evaporation of liquid drops in the core, due to the superheated vapour, helps of course to desuperheat the vapour, increase the vapour Reynolds Number, and thus increase the heat transfer from the wall.

As a drop travels towards the wall it enters the thermal boundary layer, and the temperature gradient in the layer causes differential evaporation around the drop. The larger evaporation rate on the wall side, coupled with the physical presence of the wall, leads to a differential pressure force tending to push the drop away from the wall. There are also drag and 'jet' forces acting on the drop, pushing it away from the wall. The latter component is obtainable from the rate of

change of momentum of the vapour generated, applied to a control volume whose boundary is coincident with the drop surface. However, an estimation of their effective values shows the 'jet' and drag forces to be two or more orders of magnitude less than the pressure force. The pressure force itself increases with wall superheat. Thus if the wall superheat is high enough, it will be possible to bring the drop velocity to zero and reverse it before the drop touches the wall. At low wall superheats, the drop will be able to hit the wall, and at some intermediate ΔT_w , the drop will just touch the wall. For a given G , X and P value set, there is a distribution of drop sizes and drop deposition velocities. Thus the possibility exists that at any given wall superheat, some of the drops will make it to the wall while others will not. This possibility of drop-wall contact is not restricted to any wall temperature, although at contact boundary temperatures beyond the thermodynamic critical temperature, supercritical phase changes instantaneously result upon contact. One assumption in the treatment of dispersed flow film boiling is to ignore liquid drop-wall contact. Liquid-wall contact in pool film boiling has been demonstrated by Berenson [4]. There is no reason to suppose that such contacts cannot occur in flow boiling. Thus both the drops on the wall, drops in the thermal boundary layer but not touching the wall, and the bulk vapour flow, will contribute to the total heat transferred from the wall.

THREE STEP MODEL OF DISPERSED FLOW HEAT TRANSFER

From the foregoing description, it becomes evident that heat transfer from the wall to the flow is made up of the following components:

- a) Heat transfer from wall to liquid drops which touch the wall.
- b) Heat transfer from wall to liquid drops which are in the thermal boundary layer but do not touch the wall.
- c) Heat transfer from the wall to the bulk vapour component of the two phase flow which is at the bulk vapour temperature.

A graphic presentation of the above structure is shown in figure 4. The next step is to obtain the relations for these

components.

a) Drop Contact Heat Transfer
(q/A) dc

To obtain this, one needs to know:

- i) The number of drops per unit area and time which touch the wall.
- ii) The heat transferred to a single drop touching the wall.

i) Drop deposition flux at the thermal boundary layer

As explained earlier, not all the drops entering the thermal boundary layer touch the wall. Thus we must first obtain the total drop deposition into the thermal boundary layer, and then the proportion of it which reaches the wall. In unheated flow Namic and Veda (5), parts 1

and 2, have studied drop deposition in air-water mixtures. Their results were presented in terms of it drop transfer coefficient K, as reproduced in figure 2b, and defined as

$$M = K\bar{C} \quad (1)$$

Figure 3 shows a plot of various particle disposition data from various authors, and plotted by Liu and Ilori [6]. The dimensionless deposition velocity V_i is plotted against the dimension relaxation time t_r , which is a measure of the time it takes a particle, projected into a given medium, to come into kinetic equilibrium with the environment. It is fair to

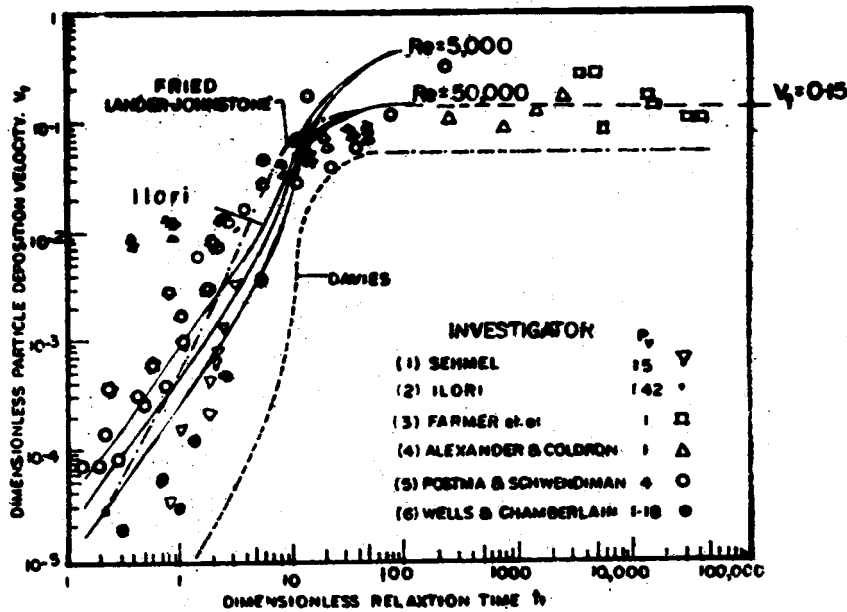


Figure 3: Theoretical and experimental particle Deposition velocities (ref. 6)

assume, from figure, that for dispersed flow with $t_t > 30$. V_i is constant at about 0.15.

Thus,

$$V_d = 0.15V^*$$

Sehmel [7] correlated V_d in terms of a penetration fraction, PF, such that

$$V_d = \frac{W_v}{\pi D \Delta Z} L_n(1/PF) \quad (3)$$

Where W_w = axial vapour volume flow rate

$$PF = \frac{\text{Particle flow rate leaving flow tub at } (Z + \Delta Z)}{\text{Particle flow rate entering flow tube at } (X)} \quad (4)$$

In dispersed flow, total mass of liquid drops entering a given cross section per unit time, is given by

$$m = G(1 - X) \frac{\pi D^2}{4} \quad (5)$$

Hence, mass M_u , deposited per unit time, is given from (3), (4), and (5) as

$$M_d = \frac{GD}{4} \frac{1-X}{\Delta Z} \frac{1^{(1-\exp(-\pi D \Delta Z V_d))}}{W_w} \quad (6)$$

Taking the limit of equation (6) as $\Delta Z \rightarrow 0$, the drop mass deposition flux M , at a cross-section where the quality is X , becomes

$$M = 0.15 \frac{(1-X)}{X} \rho_v V^* \quad (7)$$

It is possible that the deposition rate, with heat addition is influenced further by the bulk acceleration of the vapour. The possible form of this contribution is unknown, but to allow for it in very simple way, the right hand of equation (7) it multiplied by an arbitrary constant. Equation (7) then becomes

$$M = C_2 \frac{(1-X)}{X} \rho_v V^* \quad (7a)$$

Distribution of the Fraction of M which reaches the wall

The equation of motion of a drop normal to and towards the wall is given by

$$F = \frac{d}{dt} (m_\delta V_n) \quad (8)$$

where F = net force on drop perpendicular to wall. During a single traverse of the drop across the thermal boundary layer, the drop size hardly changes. Thus if the drop velocity is brought to zero at a height Y_{min} from the wall, and thermal Boundary layer thickness is Y_{b1} , then $V_n = V_d$ at $Y = Y_{b1}$; and $V_n = 0$ at $Y = Y_{min}$ so that from (8)

$$\int_{Y_{min}}^{Y_{b1}} F dY = \frac{1}{2m_\delta} V^2 d = E_{b1} \quad (9)$$

Where E_{b1} is a pseudo kinetic energy of the drop at entry to the thermal boundary layer, based on V_d . Since the drop sizes and disposition velocities are, in general, randomly distributed over the drops, it follows from equation (9) that only those drops with 'kinetic energies' at entry to the thermal boundary layer greater than or equal to a certain value, E_w , will be able to reach the wall. Thus, the probability that a drop reaches the wall is given by the probability that $(E_{b1} \geq E_w)$ or $F(E_{b1} \geq E_w)$.

A negative exponential relation is postulated flour this probability. Thus,

$$(E_{b1} \geq E_w) = e^{-aE^b w} \quad (10)$$

Where a and b are distribution constants. The expression satisfies the following limiting conditions

$$P(E_{b1} \geq 0) = 1$$

$$P(E_{b1} \geq \infty) = 0$$

It should also satisfy the definition that

$$E_m = \int_0^\infty P(E_{b1}) E_{b1} dE_{b1} \quad (13)$$

where E_m is the mean value of the distribution of E_{b1} , and $P(E_{b1})$ = probability density function = $abE^{(b-1)} e^{-aEb}$ from equation (10). Settings = E_w , equation (13) becomes

$$E_m = a \int_0^\infty s^{1/b} c^{-as} ds \quad (14)$$

The integration of equation (14) depends on the value of $1/b$ is a positive integer, integration by parts yields

$$E_m = n!/a^n (1/b = n = 1,2,3,----) \quad (15)$$

A value of $n = 1$ was chosen so that (10) becomes

$$P(E_{b1} \geq E_w) = e^{-(E_w/E_m)} \quad (16)$$

The fraction, γ of the drops entering the thermal boundary layer which reach the wall is then

$$\gamma = P(E_{b1} \geq E_w) = \exp\left(-\frac{E_w}{E_m}\right) \quad (17)$$

It is necessary to express equation (17) in terms of measured system parameters, and that can be done with the aid of equation (9) and an expression for

Table 1 – Measured Values of Thermal Conductivity of the Test Specimens

| Sample | Initial Temp. of Samples T_{s1} (oC) | Moisture Content M.C% (W.b') | Thermal Conductivity (W/m ² K) | | | | |
|--------|--|------------------------------|---|--------|--------|--------|--------|
| | | | Heat source Temperature T_h °C | | | | |
| | | | 40 | 50 | 60 | 70 | 80 |
| 1 | 10 | 59.77 | 0.0102 | 0.0010 | 0.0124 | 0.0159 | 0.0165 |
| | 30 | | 0.0105 | 0.0125 | 0.0157 | 0.0193 | 0.020 |
| 2 | 3 | 64.14 | 0.0157 | 0.0162 | 0.0165 | 0.0168 | 0.0214 |
| | 10 | | 0.0118 | 0.0155 | 0.0173 | 0.0206 | 0.0222 |
| 3 | 8 | 93.13 | 0.0150 | 0.0300 | 0.0343 | 0.0378 | 0.0412 |
| | 16 | | 0.0198 | 0.0295 | 0.0340 | 0.0417 | 0.043 |
| 4 | 5 | 70.06 | 0.0197 | 0.0242 | 0.0263 | 0.0268 | 0.0295 |
| | 15 | | 0.0121 | 0.0190 | 0.0282 | 0.0282 | 0.0325 |

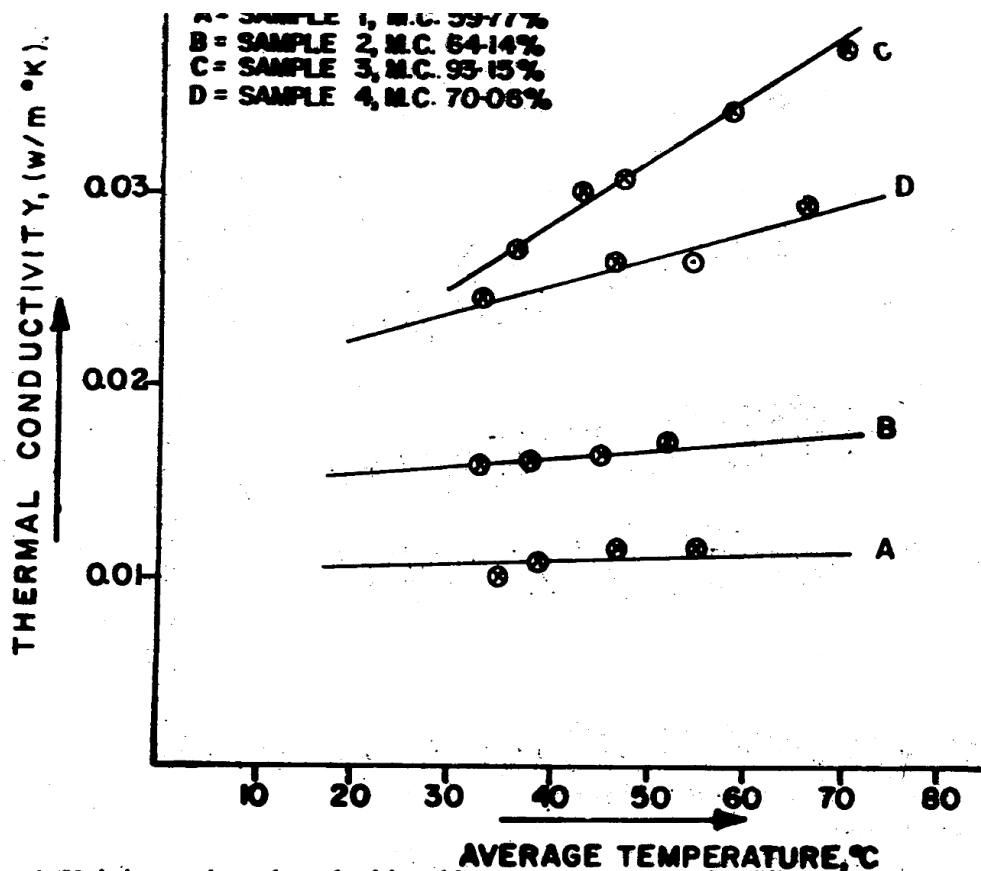


Figure 1: Variation of thermal conductivity with average temperature for different samples.

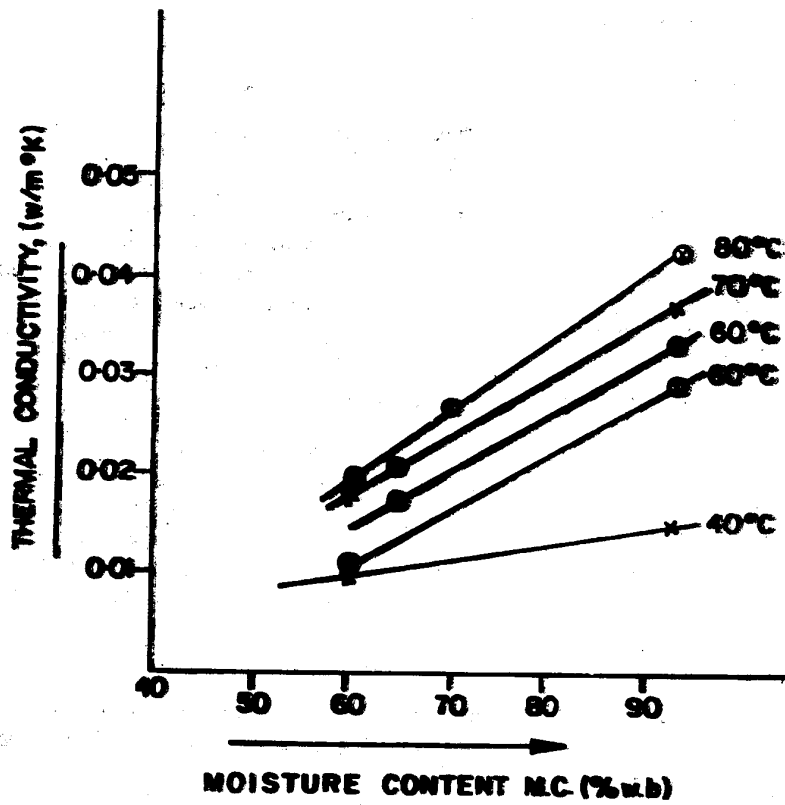


Figure 2: Variation of thermal conductivity with moisture content

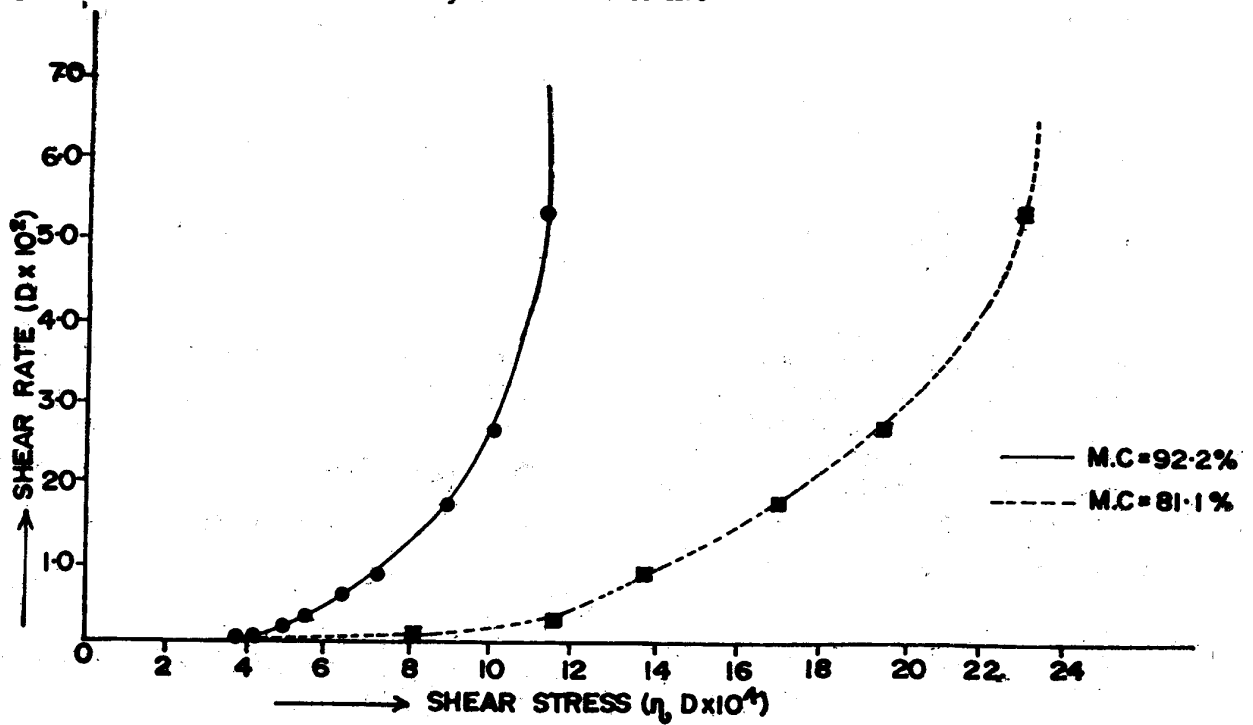


Figure 3: Variation of shear rate with shear stress

combining equations (7a) and (30), the numerical drop flux on the wall becomes,

$$N = \frac{M_y}{(\pi \rho_L \delta^3 / 6)} = 6C_2 \left(\frac{1-X}{X}\right) \rho_V V^* \frac{\exp(-\Delta T_w / \Delta T_m)}{\pi \rho_L \delta^3} \quad (31)$$

ii) Heat transferred to a single drop touching the wall

Upon impact of the saturated drop with the wall, the contact boundary temperature, T_{cb} is obtained by evaluating equation (33) at $Y=0$ and $t = 0$.

$$(T_{cb} - T_s) / (T_{wo} - T_s) = \sqrt{(kpc)_w / (kpc)_L} \quad (31a)$$

Assuming that T_{cb} is less than the temperature of limiting superheat for the liquid, at the system pressure, the following heat transfer sequence will occur, (see figure 4):

- iiia) conduction from the wall, followed by
- iiib) Nucleation and bubble growth. At end of bubble growth period the bubbles will either merge of some larger bubble will burst through the drop surface, ejecting the bulk of the liquid into the mainstream.
- iiic) Simple evaporation of liquid film left on the wall. Liquid within the interstices of the bubbles will be left on the wall. It will be too thin to support nucleation.

Event (iiib) will occur if thermal front at time of nucleation is less than liquid thickness. If not, evaporation from film surface will be the preferred event. Calculations for liquid nitrogen showed this latter process possible at qualities very close to 1. It has been possible to use a stationary drop nucleation argument because the drop axial velocities at the wall will be much smaller than the velocity of the conduction thermal front within the liquid. Heat transfer to the drop is calculated using the following assumptions:

- a) The nucleation superheat is given in [9], as

$$T_n - T_s = \frac{2R_x \sigma T_s^2}{P_L h_{fg} Y_n} \quad (32)$$

where Y_n = nucleation bubble radius = superheat layer thickness

- b) A one dimensional heat conduction model may be used to determine the temperature profile the liquid before nucleation. Thus, from Appendix 5 of [10],

$$1 - T_s = (T_{wo} - T_s) / (1 + 1) \operatorname{erfc}(Y \sqrt{(at, Lt)}) \quad (33)$$

$$1 = \sqrt{(kpc)} \text{ or } \sqrt{(kpc)} 1$$

- c) Heat transfer from wall during bubble growth in negligible
- d) The enthalpy utilized for nucleation and bubble growth is proportional to the heat transferred to the liquid superheating

period. Constant of proportionality = C_o ($C_o = 0.68$ if all heat contained in superheated layer is used for bubble generation (Appendix A7 of reference [10]).

- e) The volume of liquid left behind on the wall depends on the volume of vapour generated and may be assumed proportional to it. In reality, it depends as well on the bubble diameters and packing geometry at the end of bubble growth. For a closely packed square array of bubbles, the constant of proportionality $C_1 = 0.455$ (see reference [10,] Appendix A6).

From assumption (a) and (b) and equations (32) and (33), together with the conditions that at nucleation time t_x ,

$$Y_n = Y_x \quad (34)$$

$$(T_1)_{Y=Y_x} = T_n \quad (34a)$$

$$(\partial T / \partial Y)_{Y_x, t_x} = (\partial T_n / \partial Y)_{Y_x} \quad (35)$$

t_x may be shown to be given by

$$t_x = \left[\left(\frac{\sigma R_v T_s^2}{0.24 P_L h_{fg} \sqrt{\alpha_{t,L}}} \left(\frac{1+1}{1} \right) \right)^2 \left(\frac{1}{T_{wo}} - T_s \right)^2 \right] \quad (36)$$

The heat transferred per unit contact area during t_p is given by,

$$\phi_c = -K_L \int_0^{t_x} (\partial T_L / \partial Y_L)_{Y=0} dt \quad (37)$$

$$\phi_c = 2(T_{wo} - T_s) \left(\frac{1}{1+1} \right) \left(\frac{K_L}{\sqrt{\pi \alpha_{t,L}}} \right) t_x^{1/2} \quad (38)$$

$$\phi_c = \frac{R_v \sigma \rho_L c_L T_s^2}{0.213 P_L h_{fg}} \quad (\text{from (36) and (38) ... (39)})$$

From assumptions (d) and (e), and equation (39), heat absorbed from wall by liquid left behind, per unit contact area, is then given by

$$\phi_{Lf} = C_o C_1 \left(\frac{\rho_L}{\rho_V} \right) \frac{R_v \sigma \rho_L c_L T_s^2}{0.213 P_L h_{fg}} \quad (40)$$

A square array of equal bubbles at the end of bubble growth is most unlikely. The piercing of the liquid film by a few large bubbles is more likely so that C_1 will be greater than 0.455. Equations (39) and (40) show that except for very high pressures, ϕ_c may be neglected in comparison to ϕ_{Lf} . Thus, if δ_c is the circular diameter of the drop contact area, the heat, ψ_{dc} , absorbed by a single drop during contact, is given from (40) by

$$\psi_{dc} = C_o C_1 \left(\frac{\rho_L}{\rho_V} \right) \left(\frac{R_v \sigma \rho_L c_L T_s^2}{0.213 P_L h_{fg}} \right) \frac{\pi \delta_c^2}{4} \quad (41)$$

Combining equations (31) and (41) and

assuming δ_c to be proportional to δ , ($\delta_c = C_3\delta$), the total heat transferred from wall to drops in contact with it, $(q/A)_{dc}$ is given by

$$(q/A)_{dc} = C \left(\frac{R_v \sigma \rho_L C_L T^2 s}{0.213 P_L h_{fg}} \right) \left(\frac{1-X}{X} \right) \frac{V_v \sqrt{f}}{\delta} \{ \exp(-\Delta T_w / \Delta T_m) \} \tag{43}$$

Where $C = 0.498 C_0 C_1 C_3^2$

And f = fanning friction factor

b) Heat Transfer to Drops in Thermal Boundary Layer but Dot Touching the Wall, $(1/A)_{ndc}$

For the calculation of this component, it is first assumed that the cross-sectional void fraction is the same as the void fraction at the thermal boundary layer. Hence, fractional surface area of wall exposed to liquid = $1 - \alpha$. Proportion of liquid drops which do not touch the wall = $1 - \gamma$. If fractional surface area of wall exposed to liquid in thermal boundary layer which does not touch the wall is j , then

$$j = (1 - \alpha) (1 - \gamma) \tag{43a}$$

From equation (10) all drops with 'kinetic energy' less than E_w will not touch the wall. The average minimum trajectory height of these drops may be given by the minimum trajectory height Y_{mw} from the wall, of a drop whose 'kinetic energy', Energy E_{mw} is the mean of the distribution between $E = 0$ and $E = E_w$.

$$E_{mw} = \int_0^{E_w} E P(E) dE; \text{ where } \tag{44}$$

$$P(E) = \frac{1}{E_m} \exp(-E/E_m) \text{ from (16).}$$

From (44) we obtain

$$\frac{E_{mw}}{E_m} = 1 - e^{-E_w/E_m} \tag{45}$$

By using equation (26), it can be shown that,

$$\frac{Y_{mw}^3 E_{mw}}{\varepsilon^3 E_m} = \frac{\Delta T_w}{\Delta T_m} \tag{46}$$

From equation (29), (45)

$$Y_{mw} = \varepsilon \left(\frac{\Delta T_w}{\Delta T_m} \right)^{1/3} / [1 - \exp(-\frac{\Delta T_w}{\Delta T_m}) (1 + \frac{\Delta T_w}{\Delta T_m})]^{1/3} \tag{47}$$

For small truncation angles θ_0 , the equivalent conduction path, Y_{cp} , from a uniformly heated wall to the wall side surface of the drop, where the nearest distance to the wall is Y_{mw} , is given by (see reference [10]; Appendix A-11 for the details of calculations),

$$\bar{Y}_{cp} = 1 / \left\{ \frac{4}{\delta} \left[\left(1 + \frac{2Y_{mw}}{\delta} \right) \ln \left(1 + \frac{1}{\frac{2Y_{mw}}{\delta}} \right) - 1 \right] \right\}$$

$$(48)$$

If equation (47) is inserted into (48), the resulting equation is the equivalent conduction path at the mean or average minimum height of the drops. However, the drop starts from the thermal boundary layer, gets to the minimum height, and flies back into the main stream. The effective conduction path, $(\bar{Y}_{cp})_{eff}$ will thus be greater than \bar{Y}_{cp}

$$\text{Let } (\bar{Y}_{cp})_{eff} = \frac{1}{\lambda} \bar{Y}_{cp}$$

Where $1.0 > \lambda > 0$

Assuming a linear temperature profile across

$$(\bar{Y}_{cp})_{eff}$$

$$(q/A)_{ndc} = \lambda (1 - \alpha) (1 - \exp(-\Delta T_w / \Delta T_m)) \dots$$

$$\frac{4k_v f}{\delta} \left[\left(1 + \frac{2Y_{mw}}{\delta} \right) \ln \left(1 + \frac{1}{\frac{2Y_{mw}}{\delta}} \right) - 1 \right] \Delta T_w \tag{50}$$

where Y_{mw} = is given by equation (47)

c) Heat Transfer to the bulk Vapor, $(q/A)_{bv}$

The McAdams single phase heat transfer equation was chosen for this component. Any good single phase heat transfer correlation may be used. Since the cross-sectional void was assumed the same as the surface void, $(q/A)_{bv}$ is then given by,

$$(q/A)_{bv} = 0.023 \alpha \frac{k_{vb}}{D} Re_v b^{0.8} Pr_{vb}^{0.4} (T_w - T_{vb})$$

$$\text{Where } Re_v b = \frac{GXD}{\alpha \mu_{vb}} \tag{51}$$

And properties are calculated at bulk vapour temperatures.

Total Heat flux $(q/A)_w$

From equations (42), (50), and (51), the total heat flux becomes,

$$(q/A)_w = C \left(\frac{R_v \sigma \rho_L C_L T^2 s}{h_{fg} P_L} \right) \left(\frac{1-X}{X} \right) \left(\frac{V_v \sqrt{f}}{\delta} \right) \dots \exp \left(-\frac{\Delta T_w}{\Delta T_m} \right) + (1 - \alpha) \left(1 - \exp \left(-\frac{\Delta T_w}{\Delta T_m} \right) \right) \dots \frac{4k_v f}{\delta} \left[\left(1 + \frac{2Y_{mw}}{\delta} \right) \ln \left(1 + \frac{1}{\frac{2Y_{mw}}{\delta}} \right) - 1 \right] \Delta T_w + 0.023 \alpha \frac{k_{vb}}{D} R c_{vb}^{0.8} P r_{vb}^{0.4} \Delta T_{wv} \tag{52}$$

where Y_{mw} is given by equation (47), and X is the actual quality. Vapour superheat is allowed for in the use of ΔT_{wv} instead of ΔT_w in the heat transfer to bulk Vapour. At high wall superheats,

$$Y_{mw} = \varepsilon (\Delta T_w / \Delta T_m)^{1/3} \tag{53}$$

For the purpose of calculating heat fluxes only,

$$Y_{mv} = \varepsilon \left(\frac{\Delta T_w}{\Delta T_m} + 2.5 \frac{\Delta T_w}{\Delta T_m} \right)^{1/3} \quad (54)$$

It is to be noted that the heat transfer mechanism to the drops not touching the wall, and to the bulk vapour flow, are essentially similar, both being expressible as conduction through, an effective vapour film thickness. However the effective film thicknesses are different and whereas the sink temperature for the drops is a saturation or liquid temperature that for the vapour is at the vapour temperature, which may be superheated.

Determination of the Parameters In Equation (52)

Equation (52) then gives the total heat flux in dispersed vertical flow in terms of quantities which are calculable; given the mass flux G , actual quality X and pressure P , and in terms of the modelling parameters, $C, \Delta T_m$, and λ . C is a correlation constant. ΔT_m , however, has a specific physical significance. As will be shown later, the first component of equation (52) is predominant at low wall superheats within the boiling transition region, and may be, used to fix a value to C . At high wall superheats the first component is negligible, and if the quality is low the second component is significant. Thus λ may be fixed using the data in that region. At the minimum heat flux point the slope of the $(q/A)_w$ vs ΔT_w curve is zero, i.e,

$$\partial(q/A)_w / \partial(\Delta T_w) = 0 \quad (55)$$

Equation (55) together with minimum wall superheat data may be used to obtain values of ΔT_m .

The above procedures were carried out using data obtain with liquid Nitrogen at approximately atmospheric pressure, (references [1] and [10]). Details of the steps are given in reference [10], it is important to note that a single (G,x) set of data ($G = 40.7\text{kg/s-m}^2$ (30,000 lbm/hr-ft), $X = 30\%$) was

used to determine λ while a single value of C was used, ($C = 49.8, \lambda = 0.75$). The drop size was calculated as described in reference [10], Appendix A8. From equation (28)

$$\Delta T_m = f(G, X, \alpha, \mu_{vp}, \rho_{vp}, \rho_L, h_{fg}, \varepsilon, D, \sigma) \quad (56)$$

Using saturation instead of film temperature non-dimensional ΔT_m was plotted, as in figure (6), and correlated with the equation,

$$\frac{k_v \Delta T_m}{GD h_{fg}} = 3.27 \cdot 10^{-5} [2.93 + 4.44X + 0.084(GX/169.5)^2 - 7.35(GX/169.5)^3] / (GD/\mu_v)^{0.477} \quad (57)$$

$$40.7 \leq G \leq 169.5 \text{ Incomnel-600} \quad (58)$$

$$0.1 \leq X \leq 0.7$$

The test material for the relevant data was Inconel-600, 10.2mm id x 25mm od x 25 x 25.4mm long mounted at the top of a 2438mm preheater. The test piece was specially prepared smooth ($\varepsilon = 0.5\mu\text{m}$) as measured with a profilometer.

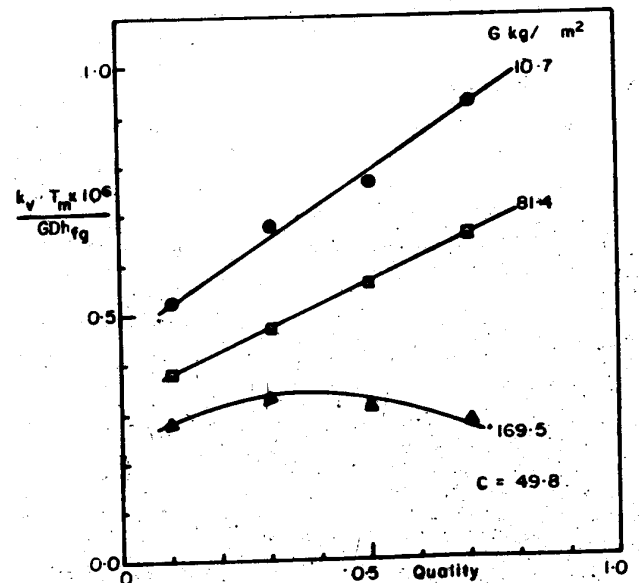


Figure 6: Dimensionless ΔT_m vs Quality.

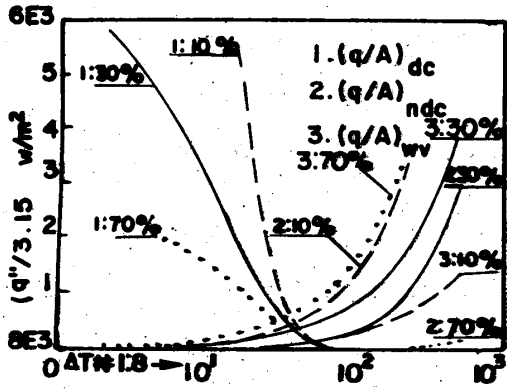


Figure 7: Effect of quality on heat flux components, components, at $G = 40.7 \text{ kg/s-m}^2$

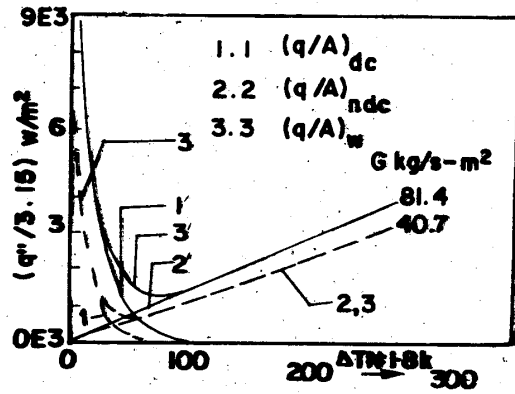


Figure 8: Effect of mass flux on heat flux at $X = 30\%$

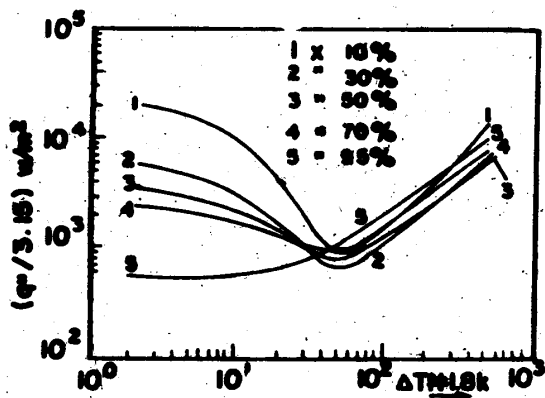


Figure 9a: Theoretical boiling curve at $G = 40.7 \text{ kg/s-m}^2$

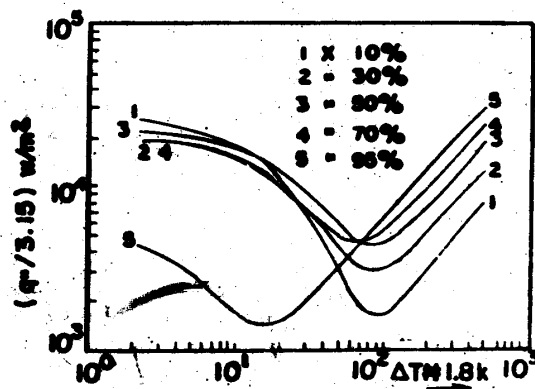


Figure 9b: Theoretical boiling curve at $G = 169.5 \text{ kg/s-m}^2$

BEHAVIOUR OF THE POST CHF BOILING CURVE (Equation 52)

(See also reference [10])

(i) Effect of Quality and Wall Superheat

Figure 7 shows the behaviour of the various components of the post critical heat flux (CHF) boiling curve, for $G = 40.7 \text{ kg/s-m}^2$ and various qualities. The drop contact heat transfer component, $(q/A)_{dc}$, is shown to be predominant at low wall superheats, and to decrease as wall superheat increases. Evidently, less drops are able to reach the wall with increasing ΔT_w . $(q/A)_{ndc}$ and $(q/A)_{bv}$ both increase with wall superheat. As quality increases, $(q/A)_{dc}$ decreases since total drop deposition falls. Also $(q/A)_{ndo}$ is very significant at low qualities, but as the total drop flux decreases with quality increasing, and as void fraction increases with quality, it becomes less than the bulk vapour heat flux component and eventually becomes negligible. Various types of simplified models, including a constant vapour film thickness, have been used in the literature for predicting heat transfer to the drops in the thermal boundary layer which do not touch the wall, $(q/A)_{nde}$. Verification of these models have however been mostly in the high quality regions. In these regions this component is very small, and the predicted heat fluxes will not be very sensitive to the model used.

(ii) Effect of Mass Flux

In figure 8, $(q/A)_{ndc}$ has been added to $(q/A)_{bv}$ and the sum plotted as a single curve. All the heat flux components increase with mass flux. The total deposition rate and the proportion reaching the wall increase with G . Vapor velocity V_v , friction factor f and T_m increase with G , hence $(q/A)_{dc}$ increases. The increased drop density in the thermal boundary layer, coupled with increased Reynolds number, also increase the other heat flux components. It should be noted that the transition region, which can be identified from the total heat flux curve, become less steep as mass flux increases. Figures 9a and 9b show the boiling curve, on conventional coordinates, for two mass flux levels and with quality as a parameter. The transition boiling regions show the expected increase in heat flux as quality decreases. Even though equation (57) is not strictly valid for $x > 0.7$, the calculation for 95% quality has been included to show what would happen as quality tends to 1. The result is not surprising. The film boiling curve merges towards the nucleate boiling region with

very flattened and almost negligible transition region. All the curves should be cut off close to the critical heat flux region. The curves also indicate that the critical heat flux decreases with quality increasing. In the higher temperature film boiling sections, a competition exists, between $(q/A)_{ndc}$ and $(q/A)_{bv}$ for predominance, with the result that for lower G 's, (q/A) tends to decrease first with increasing quality, before increasing at higher qualities.

(iii) Effect of Wall Roughness

The effect of wall roughness enters the physical model via its effect on the total deposition rate (friction factor f) and on the proportion of drops which reach the wall, γ . Both the friction factor γ increase with wall roughness and their effects to increase $(q/A)_{dc}$. The effect of wall roughness on $(q/A)_{ndc}$ is small at low wall superheats and non-existent at high wall superheats.

(IV) Effect of Contact Angle or Increase in Surface Wettability

This factor affects only the drop contact heat transfer component. The effect may be qualitatively, by referring to equation (41). Decrease in contact angle or increase in wettability, will increase δ_c and hence $(q/A)_{dc}$.

(V) Region of Validity of Equation (52)

The equation is strictly valid from the transition region, at a point where the special critical flux boiling process ceases to exist, through minimum heat flux point, to the film boiling region. At the critical heat flux point itself, it is not certain that the boiling mechanism, as described applies. In the film boiling region, the model the drop contact heat flux component does not when the contact boundary temperature is greater than the thermodynamic limiting temperature. However $(q/A)_{dc}$ is already beginning to get in that region, and whatever the actual boiling mechanism might be, the numerical values may not be very different from those obtained by extension of this model. Thus the equation may be used for the whole film boiling region.

In the prediction of post CHF heat fluxes, different correlations have been used for the three region i.e. transition, minimum heat flux and film regions. However equation 52 provides a correlation for the prediction; Since the equation is analytically based, it may be used, through differentiation, to predict the wall superheat at minimum heat flux point.

(vi) Comparison With Film Boiling Data

Figures 10a and 10b show comparison predictions using equation (52) with film data of reference [1]. The heat fluxes in the data

were very sensitive to experimental errors at lower wall superheats. Reliable data were not available in the transition boiling region so that comparison there was not possible. Otherwise the equation shows good agreement with the data. It is useful

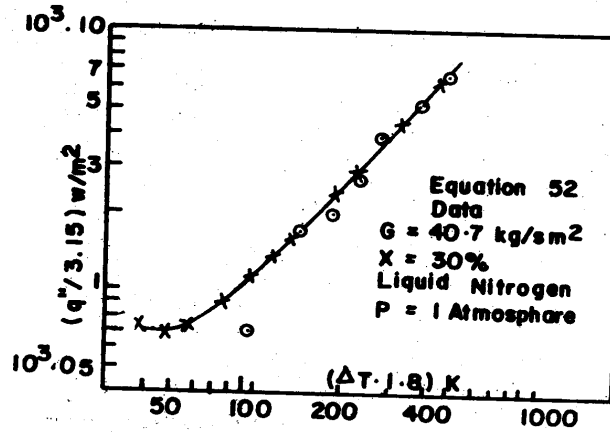


Figure 10a: Comparison of Model with film Boiling data of ref. 1, figure 30

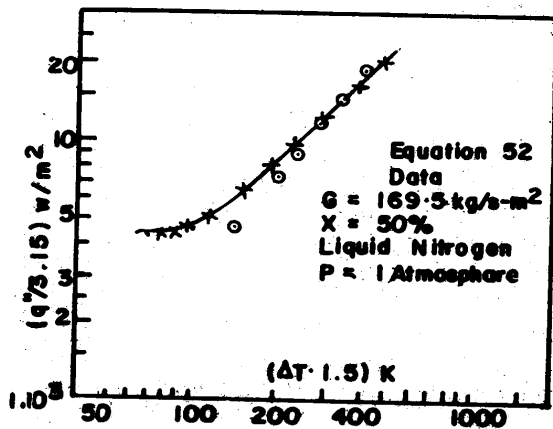


Figure 10b: Comparison of model with Film Boiling data of ref. 1, Run 119

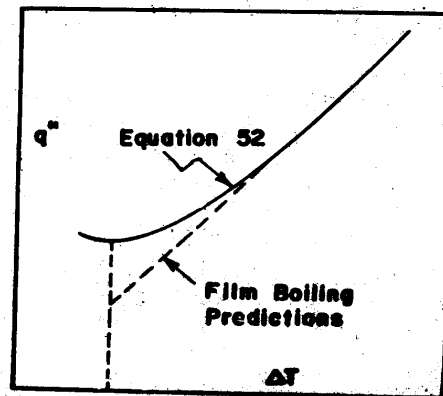


Figure 11: Difference between Model and most Film Boiling predictions.

to show the difference between the current prediction in the film boiling region with conventional film boiling predictions. This is given in figure 11.

CONCLUSION

Thus a physically based post CHF heat flux equation has been developed, in terms of most of the parameters which have been known to influence the boiling curves. Since the single model and correlation account for the transition, minimum heat flux and film boiling regions, they represent a major departure from the existing state of knowledge. Hitherto, separate models and correlations have been used for the different regions. The minimum heat flux point is clearly shown to depend on the heat transfer process itself as postulated in [11], and is not simply a function of the thermal properties of the wall and fluid. The parametric effects on the curve agree very well with known trends, When the modelling parameters have been properly tuned for liquid nitrogen the equation has compared very well with nitrogen film boiling data, and may be used through differentiation to predict the minimum heat flux point.

REFERENCES

1. Plummer, D.N., "Post Critical Heat Transfer to Flowing Fluid in a Vertical Tube", Sc.D. Thesis, M.I.T., May 1974.
2. Forslund, R.P. and Rohsenow, W.M., "Thermal Non-equilibrium in Dispersed Flow film Boiling in a Vertical Tube", M.I. T. Report No.75312 - 44, November, 1966.
3. Hynek, S.J., Rohsenow, W.M., and Bergles, A.E., "forced Convection Dispersed Vertical Flow film Boiling", M.I.T. Report No. 70586 - 63, November, 1969.
4. Berenson, P.J., "Transition Boiling Heat Transfer from Horizontal Surface", Ph.D. Thesis, M.E. Dept., MIT. 1960
5. Namie, Sadahiro and Ueda, Tatsuhiro, "Droplet Transfer In Two Phase Annular Mist Flow; Part-1", *Bulletin of the Japanese Society of Mechanical Engineers (JSME)*, No. 532529, Vol 15;, No. 90, pp, 1568-1580, 1972.
6. Liu, Y.H., and Ilori, T.W., "On the theory of Aerosol Deposition in Turbulent Pipe A University of Minnesota, Minneapolis; Particle Technology Laboratory Publication. 210, July 1973
7. Sehmel, G.A., "Aerosol Deposition from Turbulent Air Streams in Vertical Conduits", PNWL-578, pacific Northwest Laboratory, Richland, Washington, 1968.
8. Rosen, A.M ., Arr, Analysis of the Influence of Salt Concentration in Water on the Amount and Mechanism of Carry-over During Air Injection", publication of Science Academy of the Soviet Union,. No.6 1973.
9. Rohsenow W.M and Choi. N.Y., "Heat, Mass and Momentum Transfer", Prentice-Hall Inc., N.J. 1961
10. Iloeje O.C., "A study of Wall Rewer and Heat transfer is Dispersed Vertical Flow", Ph.D, Thesis, M.I.T., July 1974 Co-authors Plummer, D.N. Rohsenow W.N and Griffith. P.)
11. Iloeje, O.C., Plummer, D.N. Rohsenow, W.N, Griffith P., "As Investigation of Collags and Surface Rewer in Film Boiling in Forced Vertical Flow," *ASME J. of H, Transfer Transactions*, pp. 166-172, May, 1975